

Transition Temperatures and Critical Fields of Nb/Cu Superlattices

Indrajit Banerjee

*Department of Electrical and Computer Engineering, University of California,
Santa Barbara, California*

Ivan K. Schuller

Materials Science and Technology Division, Argonne National Laboratory, Argonne, Illinois

(Received August 11, 1983)

We present experimental results on the superconducting properties of Nb/Cu superlattices. The transition temperature of the superlattice implies a decrease in the transition temperature of single Nb films as a function of layer thickness. This is interpreted as due to the mean free path-induced decrease in the density of states at the Fermi surface, in agreement with experimentally measured magnetic susceptibilities. The temperature dependence of anisotropic critical fields is in qualitative agreement with predictions based on effective mass theories. However, the behavior of the angular dependence is considerably more complicated. In addition to the anisotropy due to the layering, there is an anisotropy due to surface superconductivity. These results are discussed in light of theories of anisotropic critical fields.

1. INTRODUCTION

The properties of artificially prepared metallic superlattices have been studied rather extensively because of the unique properties they exhibit. Among the properties that have been the focus of attention are the mechanical,¹ magnetic,² superconducting,³ transport,⁴ and piezoelectric properties.⁵ Recent impetus has been given by the development of preparation techniques with precise control over layer thicknesses, which have shown the existence of many new systems for further studies. Properties of Josephson-coupled superconducting heterostructures have been studied rather extensively, both theoretically⁶ and experimentally.⁷ However, it is found that a significant portion of the data (especially the angular dependence of upper critical fields⁸) cannot be satisfactorily explained. In this

paper we discuss mainly the superconducting properties of metallic superlattices, in particular those of Nb/Cu.

The techniques used to prepare and characterize samples have been discussed in detail in earlier papers^{3,9} and will not be discussed here. In the next section we review the zero-field superconducting properties in light of the normal state transport properties. We show that, qualitatively, the zero-field studies are in agreement with the hypothesis that the smearing of density of states reduces the T_c of Nb.¹⁰⁻¹² However, a quantitative comparison with other studies shows a lack of universal behavior. In Section 3 we discuss the superconductivity in finite fields, first the parallel and perpendicular critical fields (H_{\parallel} and H_{\perp} , respectively) as a function of temperature, and then the angular dependences. We show that proximity-coupled superlattices such as Nb/Cu behave in a similar fashion to Josephson-coupled heterostructures. However, detailed comparisons cannot be made, due to lack of proper theories in the case of proximity-coupled superconductors.

2. CRITICAL TEMPERATURES

The superconducting transition temperature T_c of 26 samples with different layer thicknesses $d = d_{\text{Nb}} = d_{\text{Cu}}$ were measured both inductively and resistively. The two measurements agreed within a few millikelvins. The results of the measurements are shown in Fig. 1.³ The transition temperatures monotonically decrease with d down to 10 Å, where they saturate at ~ 2.8 K. Calculations of T_c using the bilayer model of de Gennes and Guyon^{13,14} and Werthamer¹⁵ (dGGW) with the appropriate boundary conditions are in good agreement with the data down to a layer thickness of 300 Å (solid line in Fig. 1). Below this thickness the theory and experiment begin to diverge. Furthermore, the calculated T_c in the de Gennes version¹⁴ of the Cooper limit¹⁶ is 5.4 K, whereas the experimental saturation value

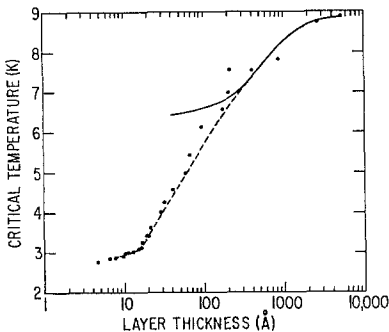


Fig. 1. The T_c of Nb/Cu samples vs. layer thickness. The solid line is the dGGW fit with no adjustable parameters. The dotted line is the dGGW fit using Nb T_c as an adjustable parameter.

is ~ 2.8 K. The apparent discrepancy between the theory and the data can be explained by assuming that T_c of Nb is decreasing with reduced layer thickness. This argument is plausible since a reduced mean free path is expected to alter the density of states $N(0)$ at the Fermi level. Independent resistivity measurements⁴ on these samples show that the mean free path l is limited by the layer thickness. Using the dGGW theory and the T_c of Nb as a fitting parameter, we extracted the T_c of Nb as a function of layer thickness. The results are in qualitative agreement with T_c measurements in single-layer Nb films of decreasing thickness¹⁷ and radiation damage studies.^{18,19} It should be noted that pure Nb foils are not easily damaged by radiation,²⁰⁻²² especially when the damaging particle goes through the foil completely. However, if the damaging particle is absorbed by the foil, T_c changes drastically,^{18,19} due to a decrease in the mean free path.

The insert of Fig. 2 shows the normal state magnetic susceptibility of three Nb/Cu samples; in all three cases the susceptibility is lower than the average value of pure Nb and Cu. This result supports the hypothesis that $N(0)$ decreases with reduced mean free path. Changes in the T_c of pure Nb films as a function of mean free path were investigated by Crow *et al.*¹⁰ and Asada and Nose.²³ In Fig. 2 we plot these results, the data of Wolf *et al.*,¹⁷ and our data calculated from the dGGW theory. Even though all these results show a decrease in T_c with mean free path, there is no sign of a universal relationship. The lack of universal relationship indicates that in different experiments different processes are operating to reduce the transition temperature. In the case of radiation damage there probably is a uniform reduction of the mean free path; in the case of single films, in addition to the decrease in mean free path, the formation of a metallic surface oxide also contributes to the depression of T_c through the proximity effect. In our case the additional anisotropy of the Fermi surface due to the layering process probably also contributes to changes in the density of states.

To determine the mean free path of the sample it is customary to assume

$$\rho l = \text{const} \quad (1)$$

where ρ is the resistivity and l is the mean free path. For Nb, $\rho l = 1.5 \times 10^{-15} \Omega\text{-m}^2$ estimated from the data of Asada and Nose.²³ Equation (1) is derived from transport theory.²⁴ For $T \ll T_F$, where T_F is the Fermi temperature, it can be shown that

$$\sigma = \frac{e^2}{12\pi^3 \hbar} \tau \bar{v}_F S \quad (2)$$

where σ is the conductivity, S the Fermi surface area, τ the scattering time,

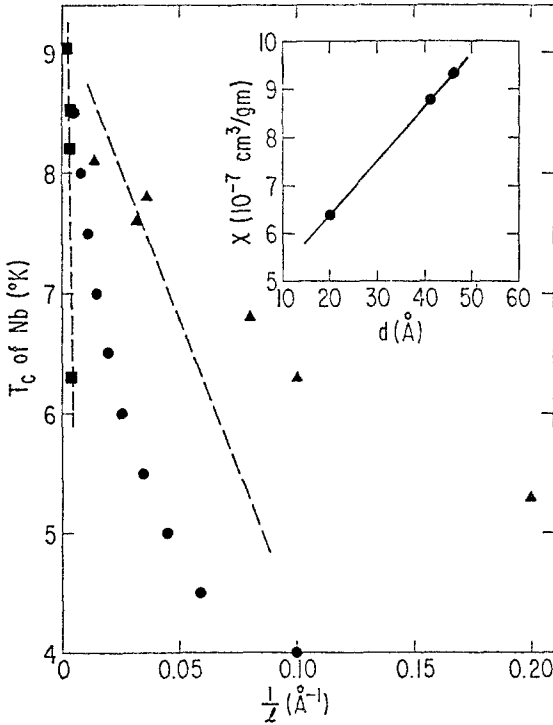


Fig. 2. Plot of T_c of Nb vs. inverse mean free path. (▲) Data of Crow *et al.* (●) Obtained from our Nb/Cu samples. (---) From the data of Asada and Nose. (■) Data of Wolf *et al.* Their mean free paths plotted here are renormalized using $\rho l = 1.5 \times 10^{-15} \Omega \cdot \text{m}^2$. The insert shows the experimentally measured susceptibilities of three Nb/Cu samples as a function of layer thickness.

and \bar{v}_F the Fermi velocity averaged over the Fermi surface. Equation (2) implies the result of Eq. (1). However, it should be stressed that τ itself could be a function of position on the Fermi surface and thus (2) has limited validity. Since the averaging procedure over the Fermi surface is not unique and because the Fermi surface area may be different in different situations, it is not surprising that no universal behavior is found.

Recent measurements on Nb/Ge heterostructure²⁵ shows that the Nb T_c inferred from extrapolating the data to zero Ge thickness is in good agreement with the T_c shown in Fig. 2.

Finally, we comment on the interfaces. In our analysis, we have assumed that interfaces are sharp, so there is proximity between pure Nb and pure Cu only. In practice there is some disordered mixture of Nb and Cu at the interface, the nature of which is not well understood. The thickness of this

“interface” is probably the same for all samples, but their relative thicknesses are not. Broadening of the central x-ray peak shows that structurally the interface has a significant effect for small layer thicknesses.⁹ Consequently, our analysis is most appropriate for large d , where the “interface” may be ignored. However, for small d , corrections ought to be made for these interfaces. A quantitative analysis of this situation is rather difficult because of the lack of detailed information on these interfaces and the lack of a suitable theoretical model.

3. CRITICAL FIELDS

Critical fields were measured resistively in a cryostat with a radial access superconducting magnet in fields up to 45 kG. The sample temperature was controlled using standard temperature control techniques and a calibrated carbon glass thermometer. The transition field is defined as the midpoint of ac resistive transition curve. Choosing the onset of resistance to be the critical field does not result in a significant quantitative change. The transitions were typically <0.3 kG wide (10–90% of the normal state resistance) at low temperatures and even less wide near T_c . Samples with layer thickness <11 Å had wider transitions and the widths have been marked in appropriate figures. It should be mentioned here that a few samples had unusually large transition fields (~ 2 – 3 kG) at intermediate angles (between 0° and 90°). A slow recovery of resistance took place after 80% of the resistance was restored.

3.1. Temperature Dependence

In an earlier paper²⁶ we showed that the samples could be classified into three categories, depending on their layer thickness. They were the following:

1. “2D, strongly coupled” region, corresponding to $d \leq 100$ Å
2. “2D, coupled” region, corresponding to $100 \leq d \leq 300$ Å
3. “3D” region, corresponding to $d \geq 300$ Å

The boundaries between these regions are not sharply defined.

In the 2D, coupled region $d < \xi_{\text{Nb}}$. Since the coherence length extends over a few layer spacings, the sample properties in this region represent an average behavior of the entire stack. In this region at low temperatures the ratio $H_{\parallel}/H_{\perp} \sim 1.7$ for all d .

For the very thick layers (3D region) $d > \xi_{\text{Nb}}$. The Nb layers are bulklike and the measured properties represent the properties of individual three-dimensional Nb layers, the copper having only a minor effect. The fact that

the ratio of H_{\parallel} and H_{\perp} is close to unity in this region implies the absence of surface superconductivity.²⁷

The most interesting region is the 2D, coupled region. In this region the coherence length of Nb can be made smaller than, equal to, or greater than d by varying the temperature. This is the region where dimensional crossover is expected to take place (as ξ_{Nb} approaches d).^{6,7} Two properties make this region unique: (1) the change in angular dependence and (2) the abnormally large ratio of H_{\parallel}/H_{\perp} at low temperatures (3.20 for $d = 171.5 \text{ \AA}$ sample at 1.17 K).

Figure 3 shows the parallel and perpendicular critical fields for a sample with layer thickness of 67.3 \AA , showing the typical behavior of all samples in the 2D, strongly coupled region. H_{\perp} is less than H_{\parallel} at all temperatures, is linear close to T_c , and tends to saturate at low temperatures—a qualitative behavior observed for all 26 samples. This is exactly the behavior expected for a bulk, type II superconductor and a thin film in a perpendicular magnetic field.²⁸ Samples with $20 \leq d \leq 200 \text{ \AA}$ have $H_{\perp}(T=0) = 12.2 \pm 1.3 \text{ kG}$. To within 10% the zero-temperature perpendicular critical fields of these samples are equal irrespective of their layer spacing. The result²⁹

$$H_{c\perp} = \phi_0 / 2\pi\xi_{\parallel}^2(T) \quad (3)$$

implies that ξ_{\parallel} is almost constant (within 10%) in this rather broad region. For samples with $d < 15 \text{ \AA}$, where x-ray lines begin to broaden, the critical fields are higher, which is typical of dirty alloys. Furthermore, close to T_c most samples show a slight positive curvature in the H_{\perp} vs. T curve, probably due to inhomogeneities in the samples. This feature was also observed by Haywood and Ast³⁰ in Al/Ge layers and Ruggiero *et al.*⁸ in Nb/Ge layers. A possible connection between the positive curvature and the Kosterlitz-Thouless transition has also been pointed out⁸; however, in agreement with

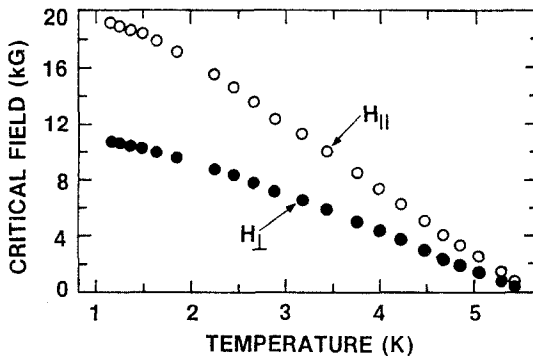


Fig. 3. Plot of H_{\parallel} and H_{\perp} vs. temperature for sample with layer thickness 67.3 \AA , which shows bulklike behavior.

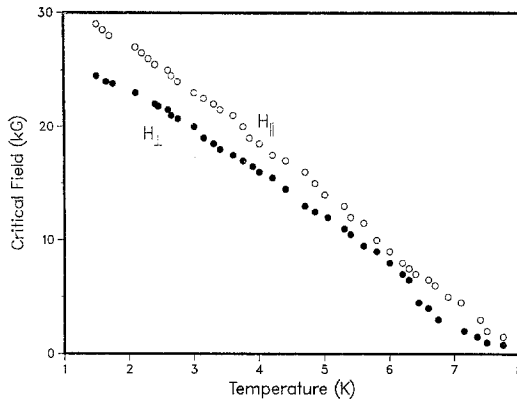


Fig. 4. Plot of H_{\parallel} and H_{\perp} vs. temperature for sample with layer thickness of 867.5 Å. The sample shows bulk-like behavior.

Haywood and Ast, we believe it to be mainly due to inhomogeneities in our samples.

The parallel critical field for a typical sample ($d = 67.3$ Å) in the 2D, strongly coupled region is also shown. H_{\parallel} is linear close to T_c and tends to saturate at low temperatures. In this region, the measured properties represent an average over many layers. In fact, the ratio $H_{\parallel}/H_{\perp} = 1.7$, is expected for a sample with an isotropic coherence length.²⁷ Conditions under which this ratio can differ from 1.69 have been discussed by Saint-James *et al.*³¹ From the observed ratio one might conclude that the coherence length of the Nb/Cu samples is isotropic in this region. The angular dependence, however, gives evidence contrary to this fact and this point will be discussed later. It should be pointed out here that the question of surface superconductivity in the presence of anisotropic coherence lengths has not been discussed in the literature and should be the subject of further theoretical work.

Samples in the 3D limit show a similar behavior (see Fig. 4). Even though the Nb layers are 3D, $H_{\parallel}/H_{\perp} < 1.69$. This latter effect is due to the proximity with the copper, whose influence is to reduce the effect of surface superconductivity. Thus in the two extreme limits (2D, strongly coupled and 3D) H_{\parallel} exhibits a behavior characteristic of bulklike samples.

The effect of layering can be seen as the temperature is reduced in samples falling in the 2D, coupled region. A dramatic upturn is observed for the sample with $d = 200.7$ Å (Fig. 5). In these samples the general feature of H_{\parallel} vs. T is that H_{\parallel} is linear close to T_c , followed by an upturn at $T = T^*$, where dimensional crossover presumably takes place; at lower temperatures there is a tendency to saturation. The upturn is representative

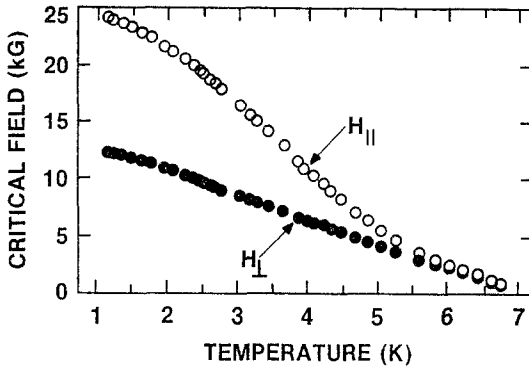


Fig. 5. Plot of H_{\parallel} and H_{\perp} vs. temperature for sample with layer thickness of 200.7 \AA . The upturn in H_{\parallel} represents the $3D \rightarrow 2D$ transition.

of a 3D to 2D transition, as discussed previously by Klemm *et al.*⁶ (KLB) and Ruggiero *et al.*⁷ At $T < T^*$, the crossover temperature, the magnetic flux preferentially penetrates the Cu, isolating the Nb layers.

In light of the discussion above, we should stress that Nb/Cu is proximity effect coupled, as opposed to systems studied previously, where the coupling was due to the Josephson effect. In fact, the present results suggest that proximity-coupled systems behave qualitatively in the same way as Josephson-coupled superconductors. A theory of superconducting layers coupled by the proximity effect is not available for comparison with our results on Nb/Cu. We should also mention that similar effects have been seen in other metallic systems. Qian *et al.*³² observed in the Nb/Ti system that two peaks occurred in the $dH_{c2\parallel}/dT$ curve, when d was equal to 15 and 200 \AA . For composition modulated layered structure, Raffy and Guyon³³ observed that, when a field is applied parallel to the layers, a peak occurs in the critical current, when the vortex lattice was commensurate with the layer spacings.

A behavior indicative of matching of the vortex lattice to the superlattice periodicity is clearly shown by a plot of the anisotropy H_{\parallel}/H_{\perp} versus layer thickness (Fig. 6). The parallel coherence length obtained from perpendicular critical field measurements is constant for all samples with $\xi_{\parallel} = 161 \pm 17 \text{ \AA}$. The peak in the parallel critical fields occurs when the layer thickness and therefore the perpendicular coherence length ξ_{\perp} is equal to ξ_{\parallel} . (We would like to thank H. Bernas for pointing this out to us.) The increase in H_{\parallel} is substantial (larger than a factor of three) and has been observed for a large number of samples.

Measurements on samples where surface superconductivity was suppressed also show similar behavior and will be the subject of a later publication.

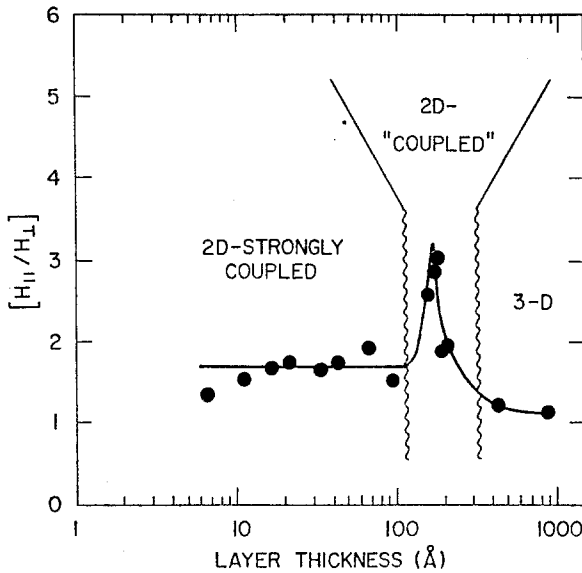


Fig. 6. Critical field anisotropy H_{\parallel}/H_{\perp} vs. layer thickness. A large anisotropy occurs when the vortex lattice is matched to the superlattice periodicity.

3.2. Angular Dependence

The angular dependence of critical fields in layered systems is not well understood. In what follows, we show that there are possibly a number of effects taking place simultaneously. Only qualitative explanations will be offered.

It is well known that thin films (thickness $d \ll \xi$) exhibit anisotropic critical fields. Based on an argument involving fluxoid quantization in thin films, Tinkham³⁴ has shown that $H(\theta)$ may be determined implicitly from the relation

$$\left| \frac{H_c(\theta) \sin \theta}{H_{\perp}} \right| + \left(\frac{H_c(\theta) \cos \theta}{H_{\parallel}} \right)^2 = 1 \tag{4}$$

Here, $\theta = 0$ corresponds to \mathbf{H} parallel to the sample surface.³⁴ Equation (4) implies a cusp in $H_c(\theta)$ at $\theta = 0$ since

$$dH_c/d\theta|_{\theta=0} = H_{c\parallel}^2/2H_{c\perp} > 0 \tag{5}$$

When there is an H_{c3} effect ($d \geq 1.8 \xi$), the experimental angular dependence is very similar to the form (4). For $\theta \rightarrow 0$ one observes H_{c3} ,

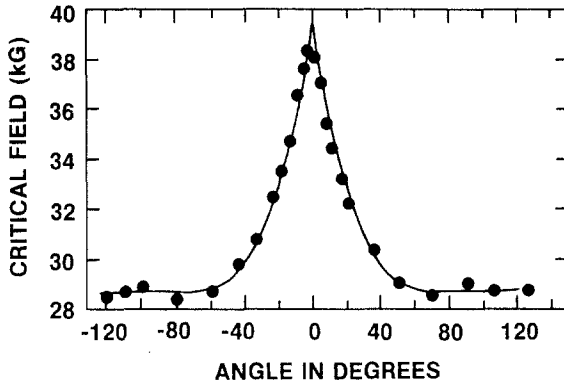


Fig. 7. Angular dependence of a pure Nb film at $T \sim 1.2$ K. Solid line is the fit to Tinkham's thin-film theory.

and as $\theta \rightarrow 90$, $H_{c3}(\theta) \rightarrow H_{c2}$.^{35,36*} Saint-James³⁷ has calculated the angular dependence of $H_{c3}(\theta)$ in terms of the initial slope $dH_{c3}/d\theta$ at $\theta = 0$. For the case of H_{c3} , the initial slope calculated is different from that of Tinkham's prediction. However, it should be noted that Eq. (4) has been seen to be valid in a number of experimental situations where there is an H_{c3} effect. In fact, we have verified that for an 8500-Å-thick film of pure Nb, the angular dependence agrees very well with the Tinkham formula (see Fig. 7). We will use this experimental fact to qualitatively describe our data. Yamafuji *et al.*³⁸ also calculated the angular dependence for the surface sheath; however, their result differs from Tinkham's by only a slight numerical amount.

For the case of layered superconductors coupled by Josephson tunneling, Lawrence and Doniach²⁹ (LD) used the Landau-Ginzburg formalism and showed that the system could be described by an "effective mass" model, i.e., as a system with an anisotropic coherence length. Since the Landau-Ginzburg formalism is generally valid only close to T_c , the LD model is expected to be valid only close to T_c . The angular dependence of the critical field can then be shown to be given by⁶

$$H_{c2}(T, \theta) = \frac{\phi_0}{2\pi\xi_{\parallel}^2(T)[\sin^2 \theta + (m/M) \cos^2 \theta]^{1/2}} \quad (6)$$

or

$$\left(\frac{H_{c2}(\theta) \sin \theta}{H_{c\perp}} \right)^2 + \left(\frac{H_{c2}(\theta) \cos \theta}{H_{c\parallel}} \right)^2 = 1 \quad (7)$$

It follows from (6) that $dH_{c2}(\theta)/d\theta|_{\theta=0} = 0$.

* $H_c(\theta)$ obtained from (4) is not monotonic for all values of H_{\parallel} and H_{\perp} . If the ratio of H_{\parallel} to H_{\perp} is $> \sqrt{2}$, $H_c(\theta)$ is monotonic. If $H_{\parallel}/H_{\perp} < \sqrt{2}$, then subsidiary minima appear between $\theta = 0^\circ$ and $\theta = 90^\circ$.

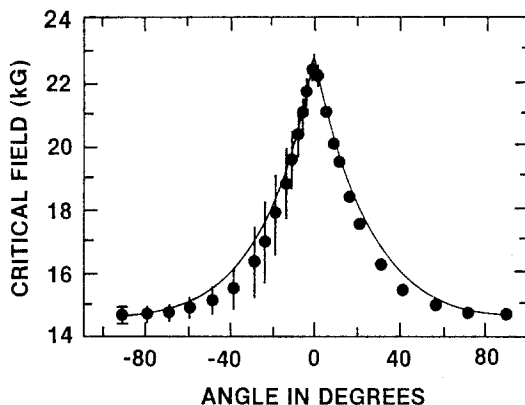


Fig. 8. Angular dependence of samples with layer thickness of 11.2 Å. The solid line is a fit to Tinkham's theory.

We should note that Eq. (6) or (7) is not directly applicable to thin films where surface superconductivity may nucleate. To suppress this effect we can imagine a situation where the magnetic field is perpendicular to a surface and the layers (direction of modulation) are inclined at an angle θ relative to the surface normal.* Such films cannot be prepared at present. Therefore, the standard techniques to determine critical fields (i.e., resistive and inductive measurements) in layered superconductors will not necessarily test the predicted LD angular dependence.²⁹ However, it will be shown that there may be a situation where the sample parameters are such that the LD dependence is closely obeyed.

Figure 8 shows the angular dependence of a sample with layer thickness 11.2 Å (corresponding to the 2D, strongly coupled region). The result is in good agreement with the Tinkham theory.³⁴ At intermediate angles, however, the transition widths of this sample were rather large and are marked in the figure. All other samples in this region show poor agreement with Tinkham's theory. The data points consistently fall below the Tinkham line (solid curves). This qualitative behavior was observed at high temperature also. These features can be distinctly seen in Figure 9, where the result is shown for a sample with $d = 16.5$ Å at two temperatures, 1.17 and 2.26 K. These results suggest that in addition to the anisotropy caused by the H_{c3} effect, there is some added anisotropy induced by the layering process. The two anisotropies, being effective at the same time, induce a larger anisotropy in the system. This extra anisotropy can be qualitatively explained by an anisotropic effective mass. An anisotropic effective mass

*This argument is due to Prof. J. B. Ketterson and we are grateful to him for pointing this out to us.

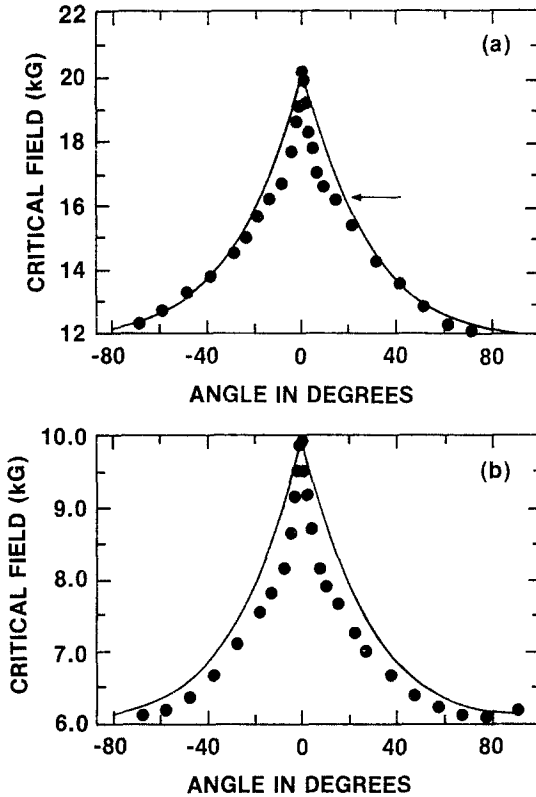


Fig. 9. Angular dependence of a sample with layer thickness of 16.5 Å. A shoulder is observed at 1.17 K (a), but disappears at higher temperatures (b).

will result in an anisotropic coherence length. The anisotropic effective mass in conjunction with the H_{c3} anisotropy will give a sharper cusp than predicted by Tinkham's theory. Since in this region the coherence lengths extend over a few layer spacings, anisotropies induced by layering are expected to manifest themselves.

There is an additional feature to be observed in the results shown in Fig. 9. There is a symmetric shoulder in the curve at low temperatures which is not present at higher temperatures. This feature was observed in almost every sample measured. This result will be discussed later.

The anisotropy exhibited by a sample of 6.5 Å layer thickness (Fig. 10) is somewhat different from the rest. The cusp is much sharper than that observed in other samples. Furthermore, there is a rise in the critical field close to the perpendicular direction. In some of the other crystalline samples,

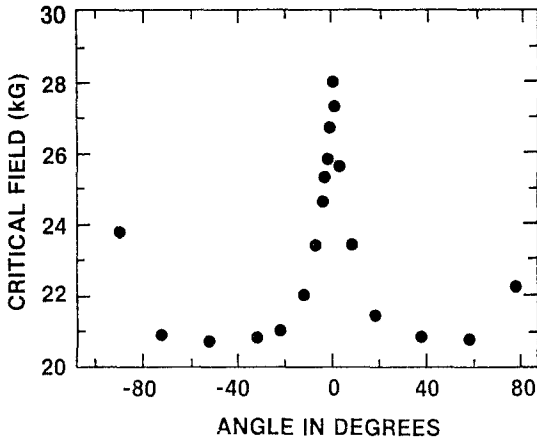


Fig. 10. Angular dependence of a sample with layer thickness of 6.5 \AA . The peak in $H_c(\theta)$ is shifted by 2.5° with H approaching H_{\parallel} from the opposite direction.

a small peak around 90° is also observed. This feature was earlier observed in pure niobium²³ and pure vanadium³⁹ films, and was explained to be a result of the columnar nature of the grains. Since the x-rays⁹ show the sample to be highly disordered, this behavior is not well understood.

Samples with large d , which fall in the 3D region, also show a cusp. But contrary to the samples with small d , the data points fall above the Tinkham line (see Fig. 11, result for a sample with $d = 420.5 \text{ \AA}$). Here the thick copper layers backing the three-dimensional niobium depress the effect of surface superconductivity and hence the anisotropy is less than

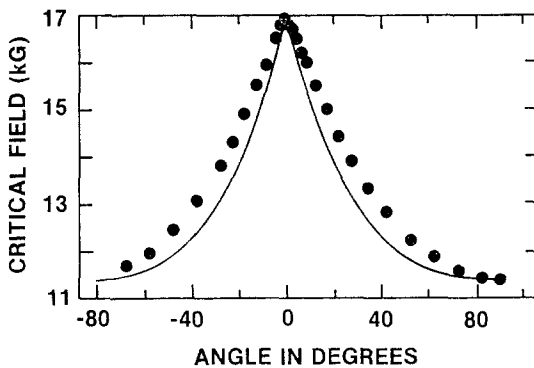


Fig. 11. Angular dependence of a sample with layer thickness of 420.5 \AA . Solid line is the fit to Tinkham's theory.

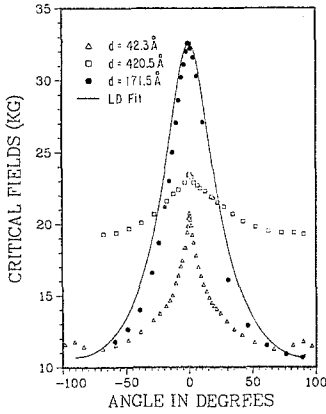


Fig. 12. Angular dependence of a sample with 171.5 Å layer thickness, showing that the Lawrence–Doniach dependence is obeyed. In contrast to the other two samples, this sample does not show a cusp. These measurements were taken at 1.17 K.

that predicted theoretically for surface superconductivity. Similar results have been observed for a sample with $d = 867.5$ Å, at two temperatures, 1.25 and 6.23 K, respectively.

We will now discuss the 2D, “coupled” region. In this region the angular dependence is highly temperature dependent. The most interesting anisotropy is shown by the sample with layer thickness of 171.5 Å (see Fig. 12). For this sample, at 1.17 K, H_{\parallel}/H_{\perp} is 3.2 and, unlike all other samples, the data do not show a cusp. Instead, the data agree closely with the theory of Lawrence and Doniach²⁹ [Eq. (7)]. Here the coupling between the layers may be such that the effective mass dominates the surface superconductivity effect. Also shown in Fig. 12 are low-temperature ($T = 1.17$ K) angular dependences for samples with $d = 42.3$ and 420.5 Å, corresponding to samples in the other two extreme limits. They clearly exhibit a cusp as opposed to the “bell”-shaped curve for the $d = 171.5$ Å sample. Since $\xi \rightarrow \infty$ as $T \rightarrow T_c$, we expect that close to T_c the layers become strongly coupled again. Interestingly, as expected, at high temperature, the angular dependence does show a cusp, the data points falling slightly below the Tinkham line. To emphasize this observation, Fig. 13 shows $dH(\theta)/d\theta$ for the $d = 171.5$ Å sample. At 1.17 K, the $\theta = 0^\circ$ slope is zero, whereas the 6.24 K slope is nonzero, clearly showing the features of a cusp. All other samples in this region, including the $d = 171.5$ Å sample at intermediate temperatures, show a feature very similar to that in Fig. 9 for the low temperature. The shoulder in different samples occurs at different angles.

From the data on the angular dependence presented thus far, and the discussion in the previous two paragraphs, it appears we are observing two effects simultaneously, namely the surface superconductivity (H_{c3}) effect and the effective-mass-type behavior. In the discussion following Eq. (7), we emphasized the conditions under which the LD dependence may be

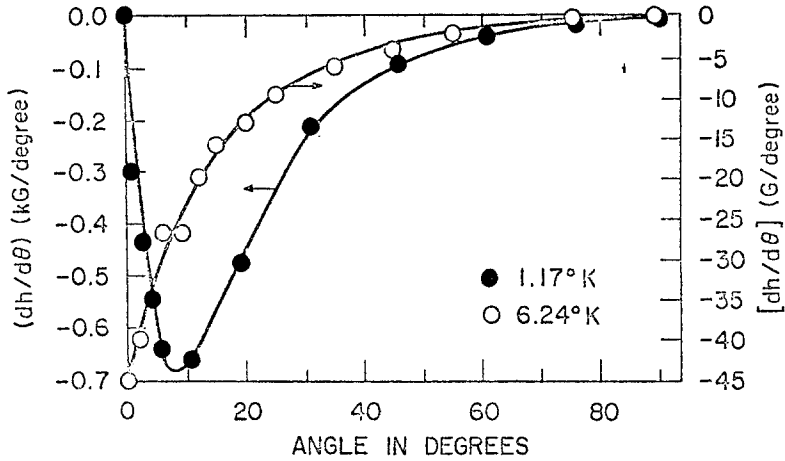


Fig. 13. Plot of $dH/d\theta$ vs. θ at two temperatures for a sample with layer thickness of 171.5 Å. The “bell”-like feature is clearly seen at low temperature, while a cusp is seen at the higher temperature.

exhibited. It is evident from the data displayed in Fig. 13 that sample parameters play an important role. We believe that for the sample with a layer thickness of 171.5 Å, the relevant parameters, d and $\xi(T)$, at 1.17 K are such that the LD dependence manifests itself more strongly than the H_{c3} effect. The large anisotropy in H_c may be thought of as arising from the nearly 2D character of the individual layers, since $H_{c2} \sim 1/d$ for a thin slab. At a higher temperature ($T = 6.24$ K) the coupling strength increases [since $\xi(T)$ increases] and what we observe is a bulk effect (of the entire sample, not the individual layers). In the limit of small d ($d \ll \xi$), the strong coupling between the layers will cause the sample to exhibit bulk-like properties under the conditions for which these experiments were performed.

We can now comment on the possibilities of detailed comparison with theory. We cannot at present make fits to the KLB theory,⁶ because that theory requires a knowledge of the effective masses. Effective masses may be determined from Eq. (6). It can be shown that

$$\left(\frac{M}{m}\right)^{1/2} = \frac{H_{c2\parallel}}{H_{c2\perp}} \tag{8}$$

or

$$\left(\frac{M}{m}\right)^{1/2} = \left. \frac{dH_{c2\parallel}/dT}{dH_{c2\perp}/dT} \right|_{T=T_c} \tag{9}$$

However, caution has to be exercised while using Eq. (9). One may use (9) close to T_c if and only if the angular dependence is given by

Eq. (6), that is, the angular dependence shows LD-type behavior. Since our angular dependence does not follow the LD behavior in general, we cannot extract the effective masses. Unless it is shown analytically how the H_{c3} and the LD anisotropy add, it is not possible at present to separate the two effects. It should be mentioned here that Choi *et al.*⁴⁰ measured the angular dependence of $(\text{TMTSF})_2\text{ClO}_4$ in the basal plane, but could not distinguish if the dependence was LD type or Tinkham type. This could also be due to the fact that they were measuring the two effects simultaneously. Unfortunately, they did not show the results of $dH(\theta)/d\theta$ to distinguish whether the data were clearly a cusp or “bell”-shaped.

Finally, we return to Fig. 9 and address the question of the symmetric shoulder in the $H(\theta)$ vs. θ curve. This feature should be compared to the smooth feature of the Tinkham line. The shoulder could be identified as a point where the flux entry occurs as the field is tipped from parallel orientations. This will be the case if one assumes the surface sheath excludes any macroscopic flux entry near parallel orientation. A transition of some sort is therefore implied. A theoretical investigation of such an effect is needed for a detailed understanding of this structure. Since almost all samples show this structure, this abrupt entry of flux may exist universally. Further investigations are under way with unequal layer thicknesses, to study in detail the coupling between the layers and the corresponding change in the angular dependence.

In conclusion, we have shown that superconducting transition temperatures of Nb/Cu samples can be explained by the proximity effect theory to small layer thicknesses provided we invoke the notion that the T_c decreases with layer thickness. This conclusion is consistent with the idea that a reduced mean free path will alter $N(0)$, hence the T_c . It is found, nevertheless, that a serious discrepancy exists among the data of various authors, which likely arises from the estimation of the mean free paths. Furthermore, we have shown that when a magnetic field is placed parallel to the layers, dimensional crossover can take place, just like in Josephson-coupled systems. Also, the angular dependence studies show that in the usual measurements two effects are observed simultaneously, namely the H_{c3} effect and the Lawrence–Doniach-type effective mass effect. How the two add is unknown theoretically and as yet unresolved experimentally.

ACKNOWLEDGMENTS

We would like to thank Dr. Gert Schön, Dr. R. Klemm, Prof. G. Deutscher, Prof. H. Bernas, and Prof. M. R. Beasley for discussions at various stages of this work. Special thanks go to Prof. John Ketterson for

his constant encouragement, questioning, and help in clarifying various theoretical points involved in this study. We would also like to thank Prof. C. M. Falco for discussions in this and related subjects, and Q. S. Yang for experimental help in the initial stages of this work. This work was supported by the U.S. Department of Energy.

REFERENCES

1. J. E. Hilliard, in *Modulated Structure—1979*, J. M. Cowley *et al.* (American Institute of Physics, New York, 1979), p. 407, and references cited therein.
2. Ivan K. Schuller and Charles M. Falco, in *Microstructure Science and Engineering/VLSI*, Vol. 4, N. Einspruch, ed. (Academic Press, New York, 1982), p. 183, and references cited therein.
3. Indrajit Banerjee, Q. S. Yang, Charles M. Falco, and Ivan K. Schuller, *Solid State Commun.* **41**, 805 (1982).
4. T. R. Werner, Indrajit Banerjee, Q. S. Yang, Charles M. Falco, and Ivan K. Schuller, *Phys. Rev. B* **26**, 2224 (1982); D. Baral and J. E. Hilliard, *Appl. Phys. Lett.* **41**, 156 (1982).
5. H. K. Wong, G. K. Wong, and J. B. Ketterson, *J. Appl. Phys.* **53**, 6834 (1982).
6. R. A. Klemm, A. Luther, and M. R. Beasley, *Phys. Rev. B* **12**, 877 (1975).
7. S. T. Ruggiero, T. W. Barbee, Jr., and M. R. Beasley, *Phys. Rev. Lett.* **45**, 1299 (1980); also see S. T. Ruggiero, Ph.D. Thesis, Stanford University, unpublished.
8. S. Ruggiero, T. W. Barbee, Jr., and M. R. Beasley, to be published.
9. I. K. Schuller, *Phys. Rev. Lett.* **44**, 1597 (1980).
10. J. E. Crow, M. Strongin, R. S. Thompson, and O. F. Kammerer, *Phys. Lett.* **30A**, 161 (1969).
11. M. Strongin, *Physica* **55**, 155 (1971).
12. C. M. Varma and R. C. Dynes, in *Superconductivity in d- and f-Band Metals* (Second Rochester Conference), D. H. Douglass, ed. (Plenum, New York, 1976), p. 507.
13. P. G. de Gennes and E. Guyon, *Phys. Lett.* **3**, 168 (1963).
14. P. G. de Gennes, *Rev. Mod. Phys.* **36**, 225 (1964).
15. N. R. Werthamer, *Phys. Rev.* **132**, 2440 (1963).
16. Leon N. Cooper, *Phys. Rev. Lett.* **6**, 689 (1961).
17. Stuart A. Wolf, James J. Kennedy, and Martin Nisenoff, *J. Vac. Sci. Technol.* **13**, 145 (1976).
18. H. Lutz, H. Weismann, M. Gurvitch, A. Goland, O. F. Kammerer, and M. Strongin, in *Superconductivity in d- and f-Band Metals* (Second Rochester Conference), D. H. Douglass, ed. (Plenum, New York, 1976), p. 535.
19. R. M. Zakirov, V. P. Kuznetsov, and T. D. Shermeger, *Sov. J. Low Temp. Phys.* **6**, 672 (1980).
20. H. Berndt and F. Sernetz, *Phys. Lett.* **33A**, 427 (1970).
21. H. R. Kerchner, R. R. Coltman, C. E. Kallunde, and S. T. Sekula, *J. Nucl. Mater.* **72**, 233 (1978).
22. G. Ischenko *et al.*, *J. Nucl. Mater.* **72**, 212 (1978).
23. Yuji Asada and Hiroshi Nose, *J. Phys. Soc. Jpn.* **26**, 347 (1969).
24. N. W. Ashcroft and N. D. Mermin, *Solid State Physics* (Holt, Reinhart and Winston, New York, 1976).
25. M. R. Beasley, private communication; S. T. Ruggiero, Thesis (1981), unpublished.
26. Indrajit Banerjee, Q. S. Yang, Charles M. Falco, and Ivan K. Schuller, *Phys. Rev. B*, **28**, 5037 (1983).
27. D. Saint-James and P. G. de Gennes, *Phys. Lett.* **7**, 306 (1963).
28. T. Kinsel, E. A. Lynton, and B. Serin, *Phys. Lett.* **3**, 30 (1962).
29. W. E. Lawrence and S. Doniach, in *Proceedings of the Twelfth International Conference on Low-Temperature Physics*, E. Kanada, ed. (Academic Press of Japan, Kyoto, 1971), p. 361.

30. T. W. Haywood and D. G. Ast, *Phys. Rev. B* **18**, 2225 (1978).
31. D. Saint-James, E. J. Thomas, and G. Sarma, *Type II Superconductivity* (Pergamon Press, Oxford, 1969).
32. Y. J. Qian, J. Q. Zheng, Bimal K. Sarma, H. Q. Yang, J. B. Ketterson, and J. E. Hilliard, *J. Low Temp. Phys.* **49**, 279 (1982).
33. Helene Raffy and Etienne Guyon, *Physica* **108B**, 947 (1981).
34. M. Tinkham, *Phys. Rev.* **129**, 2413 (1963).
35. J. P. Burger, G. Deutscher, E. Guyon, and A. Martinet, *Solid State Commun.* **2**, 101 (1964).
36. J. P. Burger, G. Deutscher, E. Guyon, and A. Martinet, *Phys. Rev.* **137**, A853 (1965).
37. D. Saint-James, *Phys. Lett.* **16**, 218 (1965).
38. K. Yamafuji, E. Kusayanagi, and F. Irie, *Phys. Lett.* **21**, 11 (1966).
39. A. S. Sidorenko, A. E. Kolin'ko, L. F. Rybal'chenko, V. G. Cherkasova, and N. Ya. Fogel, *Sov. J. Low Temp. Phys.* **6**, 341 (1980).
40. Mu-Yong Choi, P. M. Chaikin, P. Haen, and R. L. Greene, *Solid State Commun.* **41**, 225 (1982).